Energy 270 (2023) 126879

Contents lists available at ScienceDirect

Energy

journal homepage: www.elsevier.com/locate/energy

Proposal of multistage mass storage process to approach isothermal heat rejection of semi-closed S–CO_2 cycle

Enhui Sun [a,b], Hongfu Ji [a], Xiangren Wang [a], Wenjing Ma [a,b], Lei Zhang [a,*], Jinliang Xu [b]

[a] Hebei Key Laboratory of Low Carbon and High Efficiency Power Generation Technology, North China Electric Power University, Baoding 071003, Hebei, China
[b] Key Laboratory of Power Station Energy Transfer Conversion and System, North China Electric Power University, Ministry of Education, 102206 Beijing, China

ARTICLE INFO

Handling Editor: A. Olabi

Keywords:
Multistage mass storage
Semi-closed S–CO_2 cycle
Intercooling
Average temperature
Cooling process

ABSTRACT

For the semi-closed S–CO_2 cycle (SC), multistage compression with intercooling is an effective method to reduce the average temperature at which heat is rejected. However, in a limited time, the direct cooling of the large flow of working fluid in the intercooler will cause significant irreversible loss and the number of intercooling stages is limited in practical application. Referring to the idea of compressed air energy storage (CAES), this paper proposes a multistage mass storage process which is superior to intercooling. The conventional intercooler is replaced by the storage tank, and the slow cooling and mixing cooling are achieved by storing the working fluid in the tank for a long time. Since a long time cooling can effectively reduce heat exchange loss, the mass storage process has the potential to construct the multistage mass storage, which gets rid of the restriction of the number of stages and makes the heat rejection process closer to isothermal. Furthermore, the multistage mass storage process is compared with intercooling and CAES, respectively, revealing the similarities and differences between each other, and proving the performance advantages of the multistage mass storage process. The results show that the efficiency of the SC with four-stage mass storage is 1.17% higher than that of the SC with single-compression, and the efficiency of the SC with one-stage mass storage is 0.15% higher than that of the SC with two-stage intercooling. The sensitivity analysis of the key parameters of the compression process will shed lights on further improvement of the system. The multistage mass storage process proposed in this paper can also be applied to other compression fields involving variable temperature heat rejection process.

1. Introduction

The semi-closed supercritical carbon dioxide (S–CO_2) Brayton cycle is different from the closed S–CO_2 cycle in that there is a material exchange with the outside, which is reflected in the input of fuel and oxygen and the separation of water and carbon dioxide [1,2]. Semi-closed S–CO_2 cycle (SC) shows the characteristics of high efficiency, compactness and full carbon capture [3–5], which has gotten extensive attention and development in recent years. With the unique physical properties of S–CO_2 and the maximum operating temperature of nearly 1200 °C, the cycle achieves certain efficiency advantages compared with the integrated gasification combined cycle (IGCC) [6–9].

Based on the need for efficient power generation systems, researchers are constantly seeking various optimization methods to further improve cycle performance. The Carnot cycle requires that the average temperature at which heat is added or rejected of the cycle should be as high or as low as possible. Aiming for Carnot efficiency, regeneration, intercooling and reheating have been developed for the structural optimization of the thermodynamic system [10,11]. For the regeneration process of the SC, the current research has developed the multi-compressions regeneration process, which breaks through the limitation of single-compression regeneration and significantly increases the average temperature at which heat is added and thermal efficiency. Compared with single-compression regeneration cycle, the efficiency of recompression regeneration can be increased by 6.2% [12]. The reheating process can also effectively improve the cycle performance [13]. By expanding the fuel gas in stages and reheating it in between, the turbine exhaust temperature is increased, thereby increasing the average temperature at which heat is added. Allam [14] and Wen [15] found that reheating configuration yielded larger expansion ratio and compression power consumption by comparing one-stage reheating SC with no-reheating SC. Thus, the maximum cycle efficiency is slightly lower, but higher net power output is obtained.

The cooling process of the SC has the typical characteristics of the Brayton cycle. The temperature during the heat rejection process is

* Corresponding author.
E-mail address: zhang_lei@ncepu.edu.cn (L. Zhang).

https://doi.org/10.1016/j.energy.2023.126879
Received 13 September 2022; Received in revised form 2 February 2023; Accepted 4 February 2023
Available online 11 February 2023

Nomenclature

Acronyms

S-CO_2	supercritical carbon dioxide
SC	semi-closed S-CO2 cycle
IGCC	integrated gasification combined cycle
SPT	solar power tower
MS	mass storage
One-MS	one-stage mass storage
Two-MS	two-stage mass storage
Three-MS	three-stage mass storage
Four-MS	four-stage mass storage
Ic	intercooling
One-Ic	one-stage intercooling
Two-Ic	two-stage intercooling
S-Compr	single-compression
ASU	air separation unit
CPU	CO2 processing unit
LHV	lower heating value
CAES	compressed air energy storage
TR	temperature regenerative heat exchanger

Symbols

P	pressure (MPa)
T	tempreature (oC)
s	entropy (kJ·kg−1·K−1)
Q	heat input of the cycle (MW)
q	heating value per unit fuel (MJ·kg−1)
η	net cycle efficiency
w	power output or consumption (MW)
m	mass flow rate (kg·s−1)
h	enthalpy (kJ·kg−1)
v	specific volume (m3·kg−1)
α	split ratio
n	number of stages
C	compressor
S	mass storage tank
ΔT	temperature difference (oC)
ΔP	pressure drop (MPa)
Δh	enthalpy difference (kJ·kg−1)
t	time (s)
Δt	time difference (s)

Subscripts

1, 2, 3…	state points of cycle
R	regenerator
Cn	compressor Cn
P	pump
T	turbine
CO2	recycled CO2
O2	oxygen
R	regenerator
th	thermal
Syn	syngas
s	isentropic
ave,c	average temperature at which heat is rejected
Water	separated water
ic	intercooling
c	cold
in	inlet
out	outlet
dc	direct cooling
sc	slow cooling
mc	mixing cooling
CA	group A compressors
CB	group B compressors

variable [16], which makes the cooling process difficult to approach isothermal. In order to make the cycle further approach the efficiency limit, the intercooling process is usually coupled [17,18]. Through multistage compression with intercooling, the average temperature at which heat is rejected of the cycle decreases, and the heat rejection process gradually approaches isothermal with the increase of the number of compression stages [19]. Researchers have studied the S–CO_2 cycle with the intercooling process. Weiland et al. [20] found that it is beneficial to add one-stage intercooling in the compression process of dense fluid by analyzing the proposed direct-fired SC, which will reduce the compression power consumption by about 8% and improve the cycle efficiency by 0.45%. Mondal et al. [21] coupled the intercooling process to improve the low-temperature waste heat recovery performance of CO_2-based power plant, and found one-stage intercooling process can effectively improve the efficiency and maximum specific work output. In addition, researchers also compared different S–CO_2 cycle layouts including intercooling cycle. Zhu [22] and Wang [23] found that the S–CO_2 cycle with intercooling can achieve the highest efficiency by performing a comparison of simple cycle, recompression cycle, partial-cooling cycle and cycle with intercooling integrated into a solar power tower (SPT) system. Padilla [24] proved that the intercooling process of the main compressor in the recompression cycle increased the net power output and displayed the best performance through energy and exergy analysis. It can be seen that the intercooling process can effectively improve the cycle performance.

However, through the research of literature, it is found that the intercooling process applied in the closed or semi-closed S–CO_2 cycle has a limited stages, most of which are one-stage or two-stage intercooling [25,26]. This is because there are two limitations in the intercooling process. One is the limitation of compressor pressure ratio and the other is the limitation of heat exchange loss in heat exchanger. The limitation of pressure ratio is reflected that the pressure ratio of each compressor gradually decreases with the increase of the stages. According to the design principle of compressor, pressure ratio is the key factor affecting the adiabatic efficiency and polytropic efficiency of compressor. If the pressure ratio is too small, it is difficult to improve the performance of compressor [27]. The limitation of heat exchange loss is reflected that both pressure loss and heat exchange performance need to be considered in the heat exchange process. The traditional one-time cooling of the working fluid needs to release a significant amount of heat in a very short time. Especially, the mass flow of the working fluid is as high as 2000 kg/s in the SC [28–30]. And a large amount of heat exchange in a short time means a large heat exchange resistance [31], which increases the power consumption of the compressor. Based on the above limitations, the application of the intercooling process is less in the existing large scale power plants. It mostly focuses on one-stage intercooling in theoretical research, and a few in two-stage [32], up to three-stage [33]. There is still a great challenge to make the heat rejection process approach isothermal in practical application.

The limitation of pressure ratio is a common problem in the S–CO_2 cycle [34]. For example, the pressure ratio of the compressor in the SC is only about 2.4 [6,12]. In order to improve the low efficiency of the compressor caused by the small pressure ratio, for one thing, the pressure ratio of the compression process in the SC can be appropriately increased on the premise of ensuring the cycle performance. For another thing, it is a useful method to improve the working performance of components inside the compressor and reduce the friction loss as much as possible, which requires optimizing the design of the compressor.

However, due to the large heat exchange loss in the intercooling process, the number of intercooling stages in practical application is still limited, and there is still a certain gap to reach isothermal heat rejection. To solve this problem, the cooling process should have enough buffer time to avoid direct cooling in a short time. In this respect, compressed energy storage technology provides us with a new idea. In the compressed energy storage system, the electric energy is transformed into mechanical energy and thermal energy through the pre-compression of the working fluid and then stored [35–37]. There is a time difference between "storage" and "release" to meet the power demand in different periods [38]. Applying this idea to the cooling process of semi-closed S–CO_2 cycle, the heat exchange loss can be effectively reduced by prolonging the heat rejection time of the working fluid.

The study aims to further make variable temperature heat rejection process of the cycle approach isothermal and improve the thermal efficiency, thus a multistage mass storage process is innovatively proposed. The time difference is introduced to the heat rejection process of the SC, thus the working fluid can complete a long time cooling. Furthermore, the thermodynamic principle and characteristics of the mass storage process are analyzed. And it is proved that the superiority of the multistage mass storage process by comparing with the conventional single-compression and intercooling process. It is further compared with the reference compressed air energy storage (CAES) technology, and the similarities and differences between them are analyzed. Finally, for the SC with the multistage mass storage process, the sensitivity analysis of several key parameters in the compression process is carried out, which provides ideas for further improvement of the system.

2. Multistage mass storage process

In this section, the semi-closed S–CO_2 cycle (SC) is firstly described, and the multistage mass storage process proposed in this paper is introduced. Then, the thermodynamic principle and main innovations of the process are analyzed in detail.

2.1. Description of semi-closed S–CO_2 cycle

Different from the closed S–CO_2 cycle, the SC replaces the heat source of indirect heat exchange with the combustor of direct combustion, and couples the auxiliary systems based on the S–CO_2 power cycle, including fuel preparation unit and air separation unit (ASU) [1,6]. However, the conversion of heat and power of the system is mainly completed by the S–CO_2 power cycle unit. Therefore, other auxiliary systems are not considered in this paper, and the rationality of this treatment is ensured by assuming the constant input of syngas and oxygen [12].

The flow and *T-s* diagram of the SC are shown in Fig. 1, and it is a direct-fired regenerative Brayton cycle. The oxygen and syngas from the respective preparation systems are preheated by the regenerator and burned in the combustor. High-temperature and high-pressure flue gas enters the turbine for expansion (1–2), and then releases waste heat in the regenerator under the exhaust back pressure of about 3.5 MPa (2–3). During this process, water is condensed at dew point [33,39] and separated in the water separation unit. The remaining stream is basically pure CO_2. Part of the stream is sent to the CO_2 processing unit (CPU), while the majority is compressed and recycled back to the combustor to moderate the combustor outlet temperature [39]. CO_2 is firstly compressed by the compressor to near the critical pressure and taken to the ambient temperature in the cooler (5–7), and then is pumped to the highest cycle pressure (7–8). High-pressure CO_2 enters the cold side of the regenerator to absorb turbine waste heat, and finally returns to the combustor. The regenerator used for heat recovery is a multi-stream heat exchanger [15,40]. In the simulation process, the three streams are heated to the same temperature before combustion.

Studies show that the power consumption of the compressor is the largest part of the power consumption of the whole system [28]. Different from the steam Rankine cycle [41,42], the heat rejection process of Brayton cycle cannot keep a constant temperature. Intercooling process is an effective method to reduce the huge power consumption of single-compression and approach isothermal heat rejection. However, as mentioned in the previous section, there are many limitations on the direct cooling of the intercooling. In this context, the multistage mass storage process is proposed in this paper. The interstage cooling process is improved while retaining the multistage compression. The basic thermodynamic principle of this process is analyzed in section 2.2.

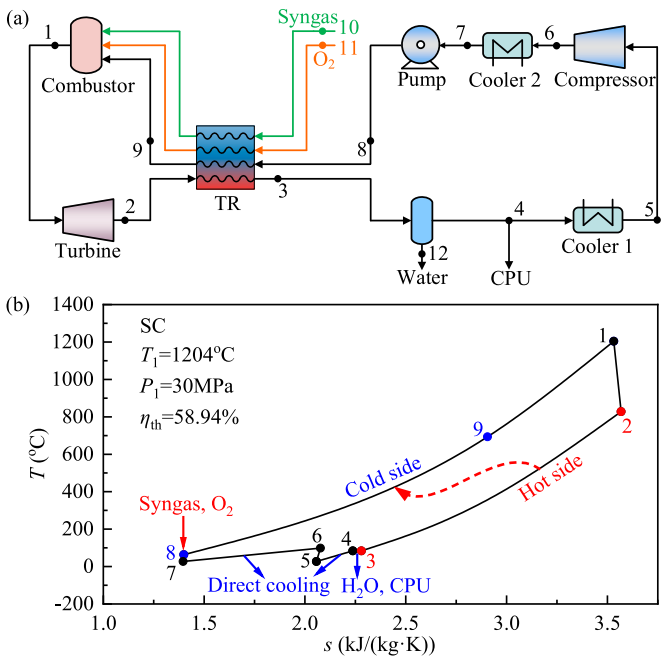

Fig. 1. Flow and *T-s* diagram of semi-closed S–CO_2 cycle (SC).

2.2. Study on thermodynamic characteristic

2.2.1. Thermodynamic principles

Fig. 2(a) shows the schematic of the multistage mass storage process. The process consists of group A and B compressors (C_1–C_{2n}) and a group of mass storage tanks (S_1–S_{n-1}). After cooling by cooler 1, the working fluid is split into two streams at point 5 and enters group A and B compressors, respectively. The working fluid at point 1′ is compressed by C_1 and then enters S_1 at point 3'. Inside S_1, the working fluid slowly releases heat to the environment to make the temperature lower than the temperature before compression, and then it is split into two streams again. One stream directly flows out of S_1 and enters C_2 for compression at point 6′, while the other stream leaves S_1 at point 4′ and is mixed with the high-temperature working fluid at the outlet of C_{n+1} (point 5′) to enter C_{n+2} together. Then compression and cooling are repeated until the final compression pressure (P_6) is reached.

In the actual process, the pressure drop in the mass storage tank cannot be neglected, which leads to the difference in the pressure ratio of group A and B compressors. In the simulation of group B compressors, the total pressure ratio is divided equally by n to ensure the same pressure ratio of from compressors C_{n+1} to C_{2n}. For the compressors of group A, pressure drop will occur when working fluid flow through the mass storage tank. In order to ensure the same pressure of the two streams to confluence and reduce the pressure loss, the outlet pressure of group A compressors is slightly higher than that of the corresponding group B compressors. The relation is as follows:

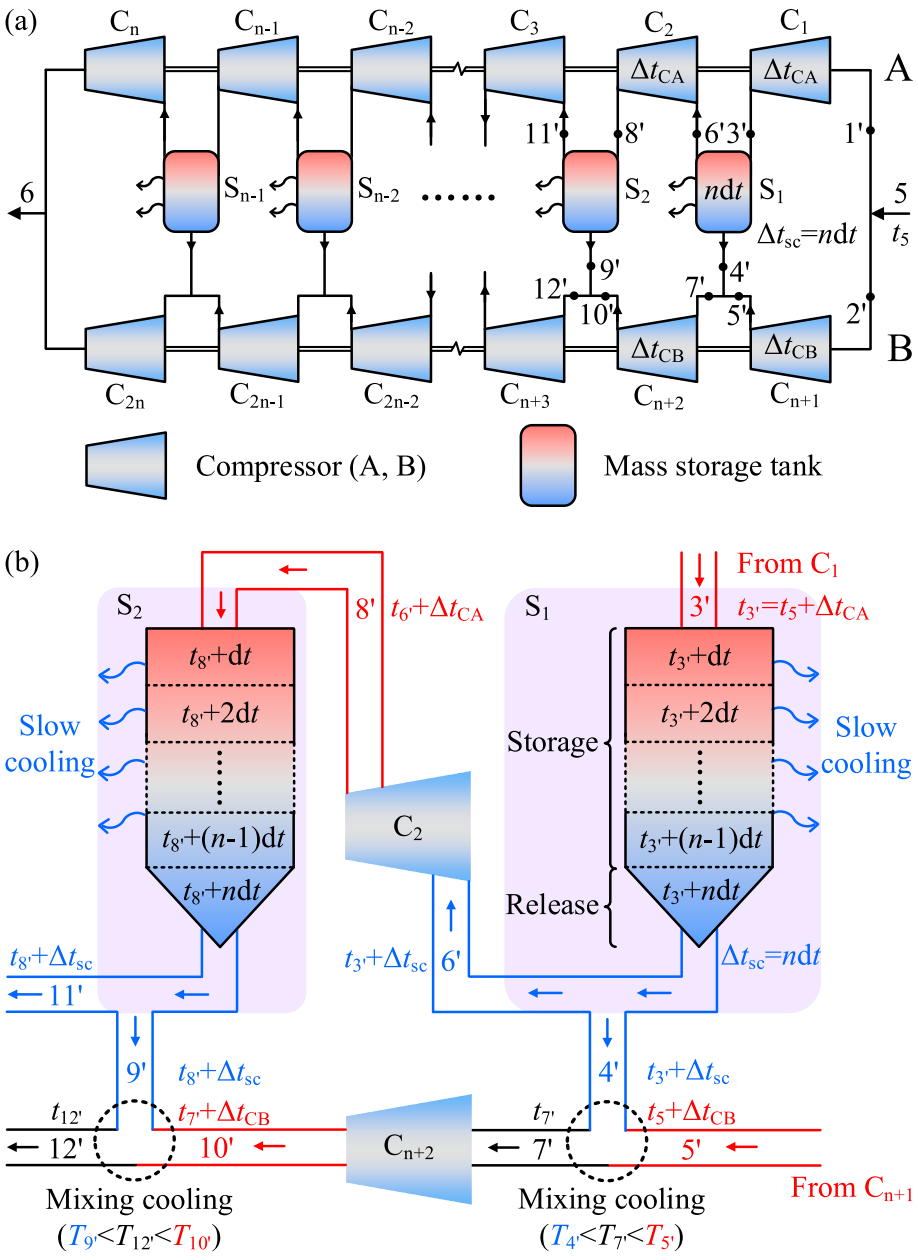

Fig. 2. Schematic diagram of proposed multistage mass storage process (Multi-MS).

$$P_{Cn,out} = P_{C2n,out} + \Delta P_S \quad (1)$$

where n ≥ 1; $P_{Cn,out}$ is the outlet pressure of group A compressors; $P_{C2n,out}$ is the outlet pressure of corresponding group B compressors; ΔP_S is the pressure drop of the mass storage tanks.

For the first time, the "time" dimension is introduced into the multistage mass storage process, and the working fluid completes "storage" and "release" processes in the mass storage tank. Fig. 2(b) is the enlarged schematic of S_1 and S_2 in Fig. 2(a). It is assumed that the compression time of working fluid in group A and B compressors is Δt_{CA} and Δt_{CB}, respectively. And the slow cooling time in the mass storage tank is Δt_{sc}. The difference of pressure ratio makes Δt_{CA} slightly larger than Δt_{CB}. The time at point 5 is t_5, and the time for the working fluid to enter S_1 at point 3′ is $t_5+\Delta t_{CA}$. Then, the time at point 4′ is $t_5+\Delta t_{CA}+\Delta t_{sc}$. In the mass storage tank, the working fluid does not complete the heat release process in a short time, but experience multiple much longer dt periods, where Δt_{sc} is equal to ndt. The working fluid has enough time to release heat to the environment, which is regarded as the "storage" of the working fluid in S_1. The "storage" process is not completed until the working fluid flows out of S_1. The working fluid leaving S_1 has two directions: point 4′ and point 6'. The high-temperature fluid compressed by C_{n+1} (point 5′, $t_5+\Delta t_{CB}$) is mixed with the low-temperature fluid at point 4' ($t_5+\Delta t_{CA}+\Delta t_{sc}$) to accomplish part of the cooling process, and then enters C_{n+2} for the next stage of compression. Therefore, the working fluids at the inlet and outlet of the mass storage tank are not synchronized in the time dimension. S_2 works in the same way as S_1, repeating the operation process of S_1.

2.2.2. *Two innovations in cooling methods*

The innovations in cooling methods of the multistage mass storage process mainly have two aspects. One is slow cooling for a long enough time. The direct air cooling or water cooling is widely used in the conventional intercooler. The heat exchange process is completed in a very short time, resulting in a large pressure drop, especially when the flow rate is high. The multistage mass storage process uses the mass storage tank instead of the intercooler to complete the heat release process to the

environment. In the mass storage tank, as a result of the existence of "storage" process, there is a large time difference between the process of "entering" and "leaving" the tank of the working fluid, and "leaving time" obviously lags behind the "entering time". In the process of storage, working fluid has plenty of time to cool, which makes the working fluid get a great buffer effect. Thus, the multistage mass storage process can realize a long time cooling which can achieve decoupling of cooling and time compared with original intercooling process. The cooling temperature can closer to the ambient temperature, and the long-time heat release can also reduce the pressure loss during the heat transfer process.

Another innovation is the mixing cooling of high- and low-temperature fluid. As for the multistage mass storage, the cooling process of working fluid is partly completed in the mass storage tank, and partly through the mixing of two streams of fluid. As shown in Fig. 2(a), for group A compressors, the working fluid enters the mass storage tank after compression and completes slow cooling. For group B compressors, the high-temperature fluid at the compressor outlet does not release heat to the environment, but is mixed with the low-temperature fluid at the tank outlet to cool. Compared with convective heat transfer in the heat exchanger, the mixing cooling significantly reduces heat transfer resistance, and reaches a higher heat transfer rate. In addition, in the calculation, the same pressure of the two streams to confluence (e.g. $P_{4'} = P_{5'}$) is ensured to minimize the confluence loss. Meanwhile, it is necessary to ensure that the temperature after each confluence is the same as the temperature of point 2' (e.g. $T_{7'} = T_{2'}$).

2.2.3. Actual operating condition

The above analysis is a detailed description of the multistage mass storage process based on design conditions. In practice, the whole process has to be flexible enough to meet the requirements of variable load under different flows and unsteady state operation. In this case, the operation of group A and B compressors is relatively independent, and they respectively play different roles. At the start-up time of the unit, a pre-stored working fluid is available in the mass storage tank, which is slowly cooled to the design temperature. With the progress of the confluence process, the working fluid in the tank is gradually reduced. At the same time, group A compressors are needed to work to supplement. Therefore, the role of group A compressors is mainly responsible for regulating the temperature and mass flow of working fluid in the mass storage tank, thereby ensuring the normal progress of the tank and the confluence process. The group B compressors run continuously to complete the process of pressure rise and cooling of the working fluid, thus reducing the average temperature at which heat is rejected of the cycle. From this point of view, group A and B compressors are decoupled. Even if the group A compressors do not work, the confluence process can be completed by the pre-stored working fluid in the tank, which does not affect the normal operation of the group B compressors. At this point, an additional mass storage tank is required at point 1′ to store the working fluid after stream splitting. If necessary, the working fluid from the storage tank can also be fed externally to increase the flexibility of the overall system.

It can be concluded that the "storage" process of working fluid is more directly reflected in the actual operation condition, providing a reference for the real operation status and regulation methods of the power plant. Moreover, considering the maturity and widespread commercial application of intercooling and compressed air energy storage technology, the multistage mass storage process is reasonable and achievable. However, this paper mainly proposes the multistage mass storage process and focuses on the thermodynamic principle and performance analysis of the system. Based on the design condition, the purpose of this paper is to study and explore the new system structure. Therefore, in the following sections, we mainly analyze the system characteristics under the design condition, without considering the operating condition under unsteady state.

2.2.4. The application of Multi-MS to SC

Fig. 3 is the flow diagram of the mass storage process, and a semi-closed S–CO_2 cycle with the multistage mass storage process is also represented in Fig. 3(d). For SC, the pressure rise is jointly accomplished by the compressor and the pump. The compressor is mainly responsible for the rising of pressure before the critical pressure, and the pump compresses the working fluid from the critical pressure to the maximum cycle pressure. In this paper, the multistage mass storage process is only used in the compressor for two reasons. Firstly, the power consumption of the compressor is greater than that of the pump in the actual cycle. Secondly, the application of the process to the pump will significantly reduce the inlet temperature of TR cold side, thereby reducing the inlet temperature of the combustor and improving the cycle heat absorption. This will undoubtedly reduce the net power output and have an adverse effect on cycle performance. To prove this conclusion, a case in which compressor with four-stage mass storage process and pump with three-stage mass storage process is simulated. The results showed a 0.061% reduction in thermal efficiency compared to applying the four-stage mass storage process only in the compressor. In summary, the multistage mass storage process is applied to the compressor in this paper to fully reveal the characteristics of the process.

2.3. Thermodynamic model

The simulation in this paper was completed by Aspen Plus. In order to be consistent with the NIST database [43], REFPROP was selected to complete the thermodynamic calculation of the cycle. The known cycle parameters are listed in Table 1. The final simulation results of SC are shown in Table 2 and each state point corresponds to Fig. 1. The calculation method refers to the textbook [44]. In addition, Appendixes A and B show the data processing process, thus the calculation results and research conclusions of this paper are credible. This section establishes the calculation model of the main components, and the cycle performance is mainly evaluated by the cycle net efficiency. Some assumptions are as follows.

(1) Assume the cycle runs in a steady state.
(2) The potential energy change of the working fluid is neglected.
(3) The pressure drops in the pipelines are neglected.

Due to the semi-closed form of the cycle, the mass flow of the working fluid always changes. For better representation, some parameters are defined. m_{Syn} and m_{O2} represent the mass flow of syngas and oxygen in the system, respectively. m_{Water} and m_{CPU} indicate the mass flow of separated water and CO_2 fluid, respectively. m_{CO2} represents the mass flow of recycled CO_2, while m_{Cn} represents the mass flow of working fluid flowing through the compressor C_n. Under the mass conservation principle of system,

$$m_{Syn} + m_{O2} = m_{Water} + m_{CPU} \tag{2}$$

The isentropic efficiency of the turbine $\eta_{T,s}$ can be expressed by its inlet and outlet parameters [12],

$$\eta_{T,s} = \frac{h_1 - h_2}{h_1 - h_{2,s}} \tag{3}$$

where h_1, h_2 and $h_{2,s}$ are the inlet enthalpy, outlet enthalpy and isentropic outlet enthalpy of the turbine in Fig. 3, respectively. The net power output w_T of the turbine can be expressed as

$$w_T = \left(m_{CO2} + m_{Syn} + m_{O2}\right)(h_1 - h_2) \tag{4}$$

where Δh_T are enthalpy differences between the inlet and outlet of the turbine. Similarly, the isentropic efficiency of the compressor and pump is respectively expressed as

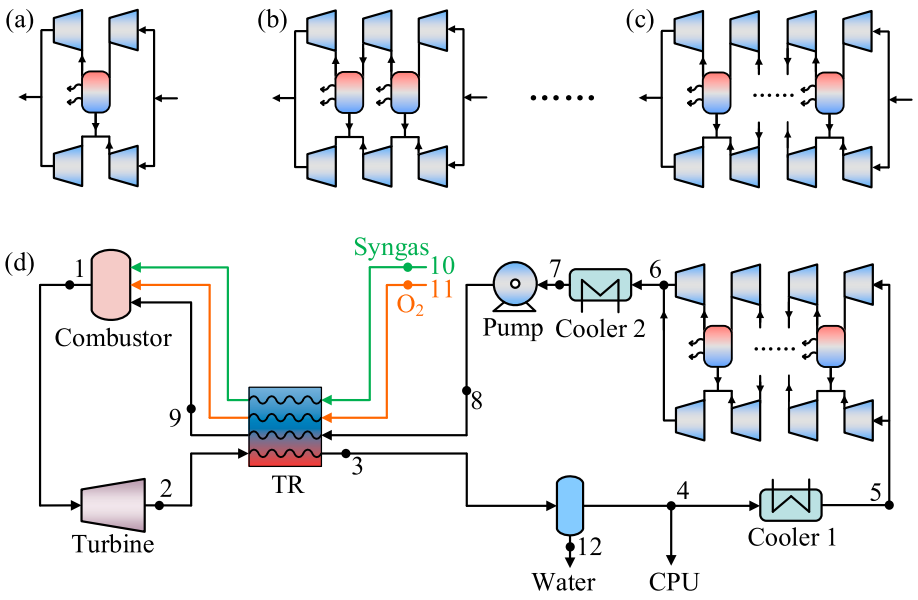

Fig. 3. Flow diagram of mass storage process (a: one-stage mass storage process, b: two-stage mass storage process, c: multistage mass storage process, d: semi-closed S–CO_2 cycle with multistage mass storage process).

Table 1
Parameters for SC simulation.

Equipment	Parameter	Value
Combustor	Outlet temperature	1204 °C [5]
	Outlet pressure	30 MPa [5,6]
Turbine	Outlet pressure	3.55 MPa
	Isentropic efficiency	0.927 [5]
Compressor	Outlet pressure	7.4 MPa [5]
	Isentropic efficiency	0.85 [26]
Pump	Outlet pressure	30.21 MPa
	Isentropic efficiency	0.85 [5]
Regenerator	Pinch temperature	20 °C
	Pressure drop	0.14 MPa
Cooler	Pressure drop	0.14 MPa [5]

$$\eta_{Cn,s}=\frac{h_{Cn,out,s}-h_{Cn,in}}{h_{Cn,out}-h_{Cn,in}} \tag{5}$$

$$\eta_{P,s}=\frac{h_{8,s}-h_7}{h_8-h_7} \tag{6}$$

considering that the multistage mass storage process includes multiple compressors, where $h_{Cn,in}$, $h_{Cn,out}$ and $h_{Cn,out,s}$ are respectively the inlet enthalpy, outlet enthalpy and isentropic outlet enthalpy of compressor C_n ($n \geq 1$). The power consumption of the compressor and pump can be expressed as

$$w_C=\Sigma w_{Cn}=\Sigma m_{Cn}\left(h_{Cn,out}-h_{Cn,in}\right) \tag{7}$$

$$w_P=m_{CO2}(h_8-h_7) \tag{8}$$

As defined by the regenerator pinch temperature ΔT_R, the outlet temperature T_3 of the high-temperature side of TR is

$$T_3=T_8+\Delta T_R \tag{9}$$

where T_3 and T_8 are the high-temperature side outlet and low temperature side inlet temperature of the regenerator, respectively [45,46].

The only heat source of this cycle is the reaction heat of syngas and oxygen, thus the heat input Q of the cycle is

$$Q=m_{Syn}q_{Syn,LHV} \tag{10}$$

where $q_{Syn,LHV}$ is the lower heating value of syngas. The average temperature at which heat is rejected $T_{ave,c}$ can reflect the heat loss at the cold source, which is defined as follows:

$$T_{ave,c}=\frac{\Sigma\Delta h_c}{\Sigma\Delta s_c} \tag{11}$$

where Δs_c and Δh_c represent the entropy difference and enthalpy difference on both sides of each cooler, respectively.

In summary, the thermal efficiency η_{th} of the SC is

Table 2
State point simulation results of the SC.

Point	Unit	CO_2	H_2O	Ar	N_2	O_2	H_2	CO	T/°C	P/MPa	Mass flow/kg/s
1	vol%	95.73	2.646	0.498	0.887	0.238	0	0	1204	30	2012
2	vol%	95.73	2.646	0.498	0.887	0.238	0	0	828.1	3.55	2012
3	vol%	95.73	2.646	0.498	0.887	0.238	0	0	83.77	3.41	2012
4	vol%	98.33	0.0058	0.512	0.911	0.244	0	0	83.77	3.41	1989.8
5	vol%	98.33	0.0058	0.512	0.911	0.244	0	0	27	3.27	1851
7	vol%	98.33	0.0058	0.512	0.911	0.244	0	0	27	7.26	1851
9	vol%	98.33	0.0058	0.512	0.911	0.244	0	0	693.4	30.07	1851
10	vol%	44.44	0.14	0.16	0.63	0	27.96	66.66	72.86	30.21	94
11	vol%	0	0	0.44	0.06	99.5	0	0	72.86	30.21	67
12	vol%	0	100	0	0	0	0	0	83.77	3.41	22.19

$$\eta_{th}=\frac{w_T-\Sigma w_{Cn}-w_P}{Q}=\frac{(m_{CO2}+m_{Syn}+m_{O2})(h_1-h_2)-\Sigma m_{Cn}(h_{Cn,out}-h_{Cn,in})-m_{CO2}(h_8-h_7)}{m_{Syn}q_{Syn,LHV}} \quad (12)$$

In order to verify the accuracy of the model, the baseline case in literature [6] is reproduced. Different from the cycle shown in Fig. 1, the turbine cooling model and the intercooling process are added to the reference case, and there are differences in the initial parameters of fuel and oxygen. Since some parameters in the reference model are not revealed, the simulation results in Table 3 are slightly different from the reference model. It can be seen that the results of model verification are satisfactory, thus the subsequent calculated data are credible and can support the interpretation of the results and research conclusions.

3. Advantages of Multi-MS

3.1. Advantages of Multi-MS over single-compression

As shown in Fig. 4, the ideal multistage mass storage process is compared with the single-compression process on the *T-s* diagram, which clearly expounds the thermodynamic principle of performance advantages of multistage mass storage process. This process obviously reduces the average temperature at which heat is rejected of the cycle. And as the number of compression stages increases, the outlet temperature of each compressor gradually decreases, and the whole heat rejection process is closed to isothermal.

From the quantitative perspective, Fig. 5 demonstrates the performance advantages of the multistage mass storage processes. Four cases of one-stage, two-stage, three-stage and four-stage mass storage processes are set up, and their performance differences with the single-compression process are compared. As can be seen from Fig. 5, the multistage mass storage process can significantly reduce the compression power consumption and the average temperature at which heat is rejected, thus improving the cycle efficiency. In the calculated case, compared with the single-compression cycle, the compression power consumption of the four-stage mass storage cycle is reduced by 16.47 MW, resulting in a 1.17% increase in cycle efficiency. In addition, the more compression stages, the more noticeable the performance advantage. However, the increment of efficiency is gradually smaller, which is the same as the principle of conventional intercooling process.

3.2. Advantages of Multi-MS over intercooling

The multistage mass storage process is proposed based on intercooling process, and they have both similarities and differences. The similarities are reflected by splitting the compression process into multiple compression units with small pressure ratio in the thermodynamic principle of their performance advantages over single-compression. The average temperature at which heat is rejected can be effectively reduced and the cycle efficiency can be improved. Both multistage mass storage and intercooling are composed of multistage compression and interstage cooling, both of which are a method to make the heat rejection process approach isothermal.

Meanwhile, there are some differences between multistage mass storage and intercooling, mainly reflected in the cooling process. Fig. 6 makes a qualitative comparison between them. Although both require the release of compression heat, they do so in different ways. For the intercooling process, the compressed high-temperature working fluid enters the cooler at one time and releases the heat in a short time. In SC, the direct cooling has the characteristics of large flow rate and short duration, which will yield large heat load and pressure loss. The multistage mass storage process improves direct cooling with a cooling process that includes slow cooling in the tank and mixed cooling, as shown in Fig. 6(c). As mentioned in section 2.2, under the same stages with the intercooling cycle, the cycle with mass storage process can realize a long time cooling which can achieve decoupling of cooling and time. Therefore, the cooling temperature can closer to the ambient temperature. In a long period of time, the velocity of the fluid can be regarded close to zero with small heat transfer resistance, thus reducing the pressure loss during the heat transfer process. Meanwhile, due to decoupling of cooling and time, the mass storage process has the potential to construct the multistage mass storage process, which gets rid of the restriction of the number of compression/intercooling stages and makes the cooling process closer to isothermal heat rejection. In addition, part of the cooling effect is also reached through the mixing of high- and low-temperature fluids. Compared with direct cooling in the intercooling process, the method of slow cooling combined with mixing

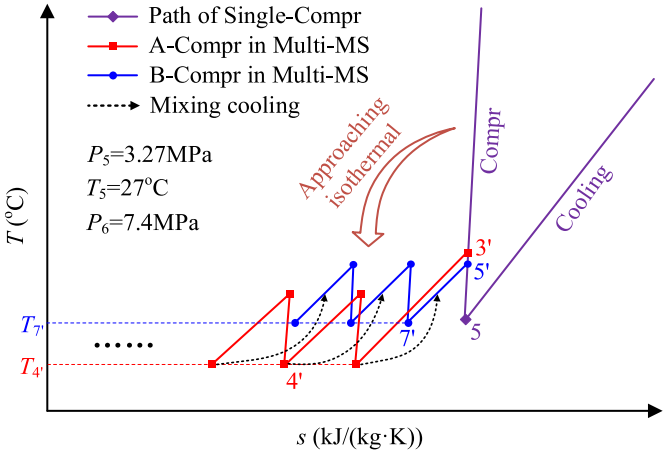

Fig. 4. Comparison of Multi-MS and single-compression on *T-s* diagram.

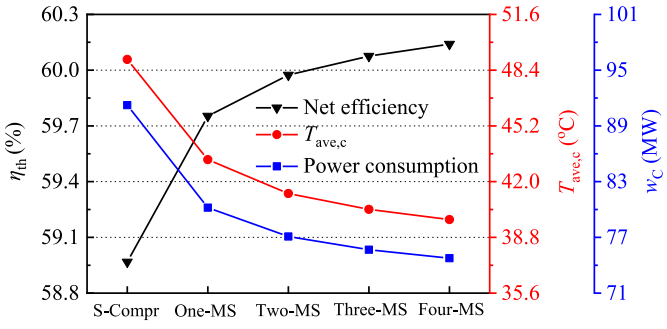

Fig. 5. Performance advantages of Multi-MS.

Table 3
Validation of model methods.

Parameters	Simulation	Literature [17]
Heat input of the cycle (MW)	1260	1260
Gross power output (MW)	934.84	926.6
Power consumption of compressors (MW)	72.25	70.5
Power consumption of pump (MW)	75.25	67.3
Net power output (MW)	787.34	788.8
S–CO_2 power cycle efficiency (%)	62.49	62.60

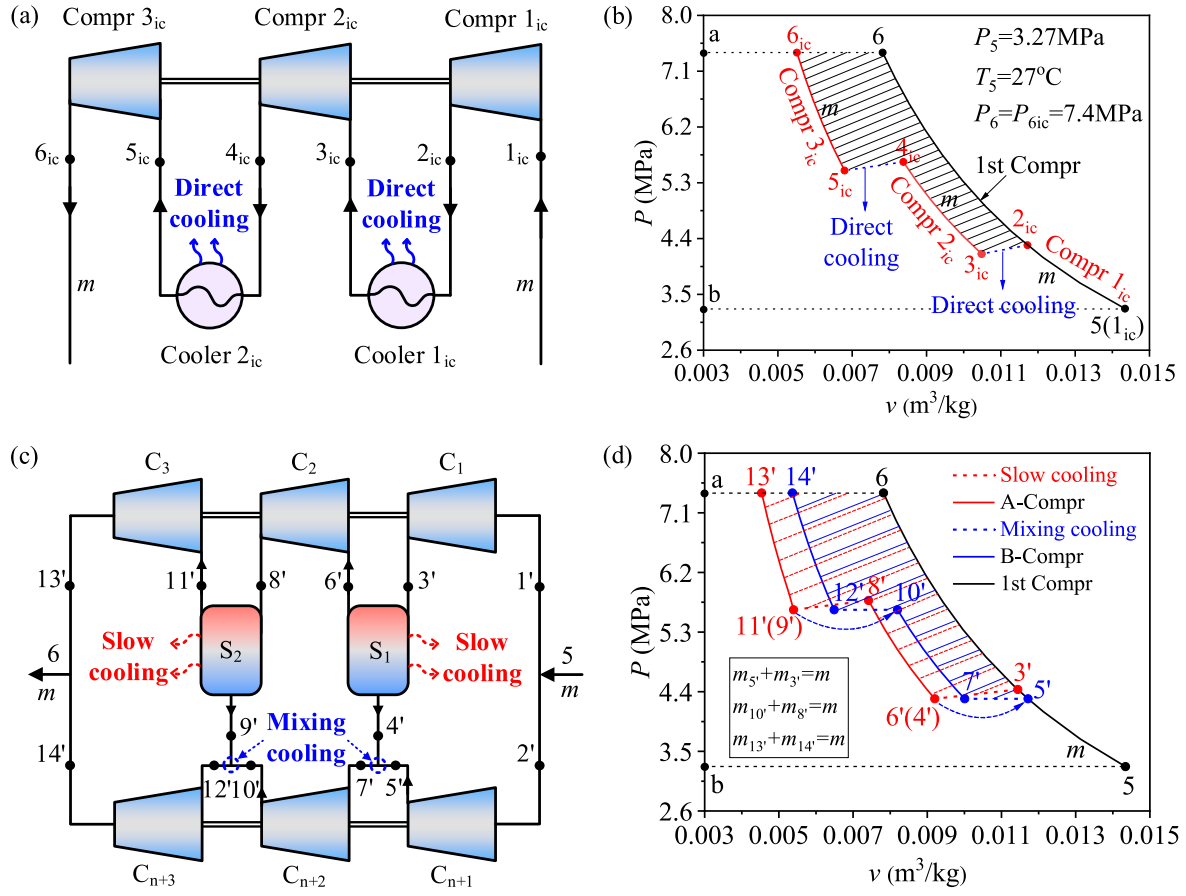

Fig. 6. The differences between Two-Ic and Two-MS (a & b: schematic and *P-v* diagram of Two-Ic, c & d: schematic and *P-v* diagram of Two-MS).

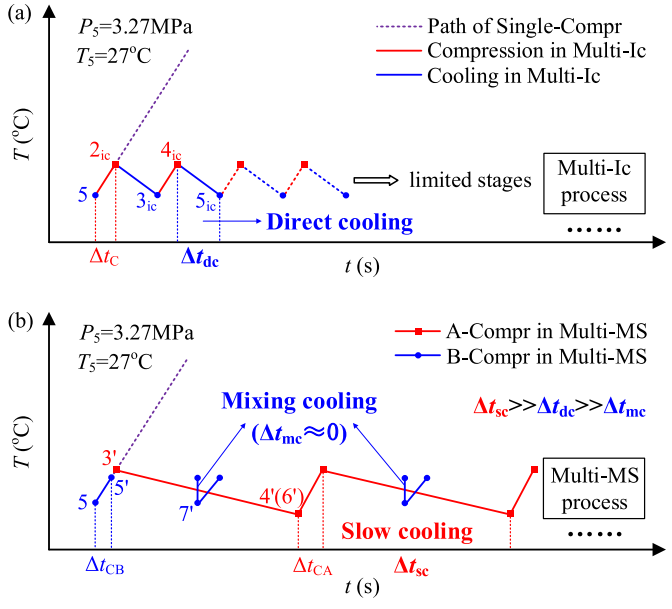

Fig. 7. Comparison of Multi-Ic and Multi-MS on *T-t* diagram.

cooling achieves the same cooling effect and pays a lower cost. In this way, the multistage mass storage process can implement more stages of compression under the premise that the system can bear the complexity. Fig. 7(a) and Fig. 7(b) represent the multistage intercooling process and the multistage mass storage process on the time scale, respectively. The abscissa is time and the ordinate is temperature. Fig. 7(b) corresponds to Fig. 2. It is assumed that the time of direct cooling, slow cooling and mixing cooling of working fluid are Δt_{dc}, Δt_{sc} and Δt_{mc}, respectively. It can be known that Δt_{sc} is much larger than Δt_{dc}, and Δt_{mc} is approximately zero. Fig. 7 clearly shows the time comparison of the three cooling methods through the *T-t* diagram and highlights the advantages of the multistage mass storage process.

The discrepancy between intercooling and mass storage process is also reflected in the mass flow. The intercooling process has only one stream with a mass flow of m_{CO2}, which flows through each compressor and cooler in turn. In the mass storage process, the initial stream split divides m_{CO2} into m_{CA} and m_{CB}. With the process of mixing cooling, m_{CA} decreases and m_{CB} increases. Although the mass flow of working fluid changes all the time, the sum of m_{CA} and m_{CB} is always m_{CO2}. According to the physical meaning of the *P-v* diagram, the shaded area between two curves represents the difference of their power consumption. In Fig. 6

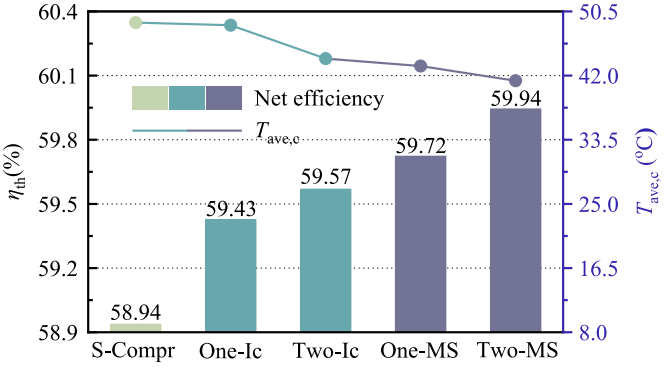

Fig. 8. Performance comparison of intercooling and mass storage process.

(b), the shadow area multiplied by the mass flow of the working fluid is the power consumption reduction of the intercooling process compared with the single-compression process. In Fig. 6(d), the two-stage mass storage process is divided into multiple parts according to the different mass flow. In each part, the power reduction of the mass storage compared with single compression is still equal to the shadow area multiplied by the corresponding mass flow, and the sum of which is the total power reduction.

Fig. 8 compares the performance of one-stage intercooling cycle, two-stage intercooling cycle, one-stage mass storage cycle and two-stage mass storage cycle, which are evaluated by cycle efficiency and the average temperature at which heat is rejected. It can be seen that the mass storage process has obvious performance advantages compared with the intercooling process. Even the one-stage mass storage cycle is 0.15% more efficient than two-stage intercooling cycle due to the mass storage process can reduce the average temperature at which heat is rejected to a much lower value, as shown in the $T_{ave,c}$ curve in Fig. 8.

3.3. Comparison of Multi-MS and CAES

Compressed gas energy storage is to use the remaining power for compressed gas at low grid load. At high grid load, the compressed gas is released to drive the turbine for power generation [35,47]. The existing compressed air energy storage (CAES) technology is sophisticated that has achieved large-scale commercial applications. Fig. 9 is a simple schematic of the CAES system. During the charge process, ambient air is compressed to high-pressure by intercooling process and then stored in a storage tank. During the discharge process, the high-pressure air released from the storage tank enters the turbine to generate electricity through the multistage reheating process. For the CAES system, the heat storage medium is water, which transfers the compression heat to the multistage reheaters through an independent water cycle.

The principle of multistage mass storage process borrows the characteristics of CAES. The existence of storage tank makes the working fluid has a storage process, which reflects the similarity between Multi-MS and CAES. However, in some aspects, there are obvious differences of them, as shown in Fig. 10. Firstly, they have different storage medium. CAES is based on the storage of air, but in fact it stores the high-pressure energy of air. And the storage location is after the intercooling process. The multistage mass storage process is completely the storage of fluid medium, and the storage process exists in each stage of the compression process. Secondly, their purposes are different. Due to the existence of "storage" and "release", both of them introduce the "time" concept. The CAES uses the time difference to match the power grid load demand at different times, while the multistage mass storage introduces time difference to prolong the heat release time of working fluid.

Finally, there are discrepancies in the release object and the final destination of compression heat. As for CAES, the compression heat of air is released to the water in the intercoolers, which then supplies heat to the cryogenically expanded exhaust gas, thus the compression heat is reused. As for the multistage mass storage process, the working fluid carrying the compression heat enters the mass storage tank and the heat is released to the environment by slow cooling. As a result, its compression heat is discarded without recycling. Meanwhile, they have a different flow of mechanical energy. For CAES, the high-pressure air stored in the storage tank is released and directed to the multistage expanders, where the mechanical energy is used to drive the turbine to generate electricity. By contrast, for Multi-MS, after the fluid in the mass storage tank releases heat, it is mixed with high-temperature fluid at the outlet of the tank, thus the mechanical energy is utilized for the inter-stage mixing cooling.

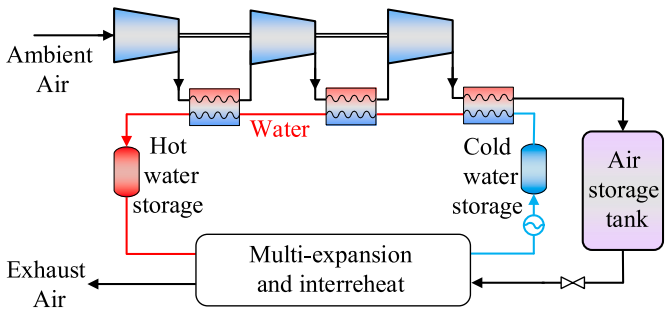

Fig. 9. Simple schematic diagram of compressed air energy storage (CAES).

4. Sensitivity analysis

According to the calculation assumptions in section 2.3, the SC is firstly simulated in Aspen plus. In this system, the compressor adopts single-compression, and the cycle performance is given in Table 4. All subsequent sensitivity analyses are based on the SC.

4.1. Influence of initial split ratio on cycle performance

As mentioned in section 2.2, the pressure ratio and intermediate cooling temperature of the group A and B compressors are different, thus the mass split ratio at point 5 is the key factor affecting the compression power consumption. In this section, four cases of one-stage mass storage cycle (One-MS), two-stage mass storage cycle (Two-MS), three-stage mass storage cycle (Three-MS) and four-stage mass storage cycle (Four-MS) are set to study the impact of different mass storage stages on cycle performance.

It is assumed that the mass flow of working fluid flowing through the group A compressors after stream splitting is m_{CA}, and that flowing through group B compressors is m_{CB}. The split ratio α is defined as the ratio of m_{CA} and $m_{CA} + m_{CB}$,

$$\alpha = \frac{m_{CA}}{m_{CA} + m_{CB}} \tag{13}$$

where $m_{CA} + m_{CB} = m_{CO2}$, $0 < \alpha \leq 1$. Notice that α is not infinitely close to zero. The value of α shall ensure the constant temperature after confluence. If α is very small, in the subsequent process, even if all the fluid from the tank participates in the confluence, it is still not enough to lower the high-temperature fluid to the design temperature. Therefore, there is a lower limit α_{min} of α, and the α_{min} is different in different cases. As α increases, a smaller proportion of working fluid in the mass storage tank flows to the confluence. Therefore, the maximum value of α is 1 (i.e., all the working fluid flows through group A compressors). However, the larger the α, the larger the volume and capacity of the mass storage tank, which makes the economy worse to some extent. The purpose of this section is to investigate the effect of split ratio on cycle performance and to determine the maximum efficiency in each case. Table 5 lists the values of α in different cases.

Fig. 11 shows the variation of cycle efficiency and compression power consumption with α in four cases. It reveals that the four curves show similar trends. With the increase of α, the total compression power consumption decreases gradually, and the cycle efficiency constantly improves. That is because the lower initial compression temperature can make the compression end closer to the critical value, which can greatly reduce the compression power consumption for CO_2 working fluid. The increase of α means that m_{CA} increases and m_{CB} decreases. Thus, the cycle efficiency is proportional to α in the final effect. Fig. 11 indicates the maximum efficiency of the four cases, all of which are all obtained when α is equal to 1. At that time, the working fluid no longer flows through group B compressors.

4.2. Influence of key parameters on cycle performance

To grasp a better idea of cycle performance, this section shows a sensitivity analysis of several key parameters of the cycle. In the SC, the

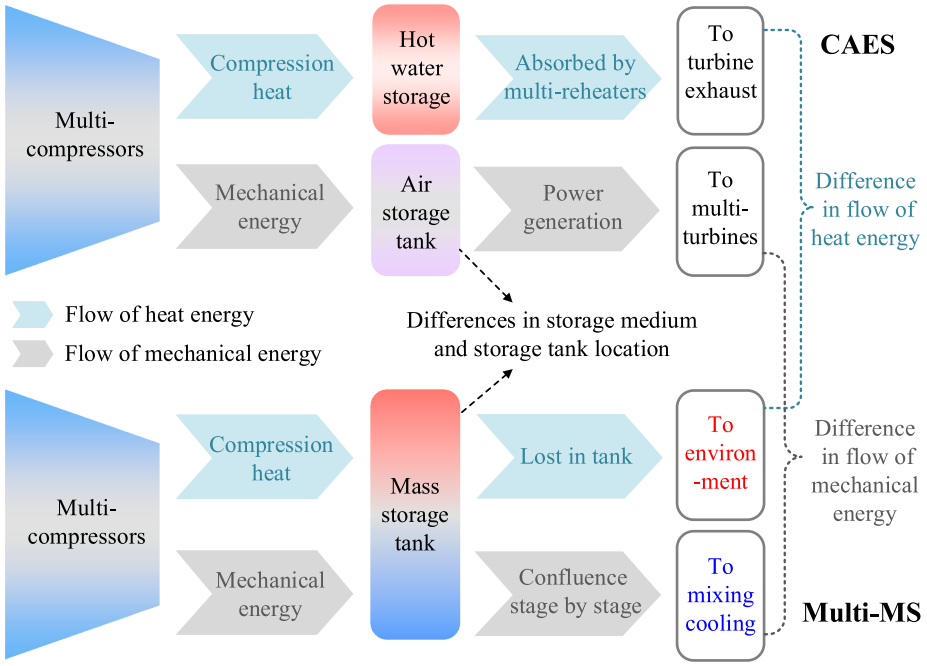

Fig. 10. The differences between CAES and Multi-MS.

Table 4
Overall performance summary of SC.

Parameters	Unit	Value
Mass flow of recycled CO_2	kg/s	1851 [5]
Heat input of the cycle	MW	1404.8
Gross power output	MW	999.46
Power consumption of compressor	MW	91.23
Power consumption of pump	MW	80.29
Net power output	MW	827.94
S–CO_2 power cycle efficiency	%	58.94

Table 5
Variable condition setting of α under different cases.

Cases	Variation of α				
One-MS	0.7468	0.8101	0.8734	0.9367	1
Two- MS	0.8824	0.9118	0.9412	0.9706	1
Three- MS	0.9346	0.95095	0.9673	0.98365	1
Four- MS	0.9634	0.97255	0.9817	0.99085	1

compression process is divided into a compressor and a pump. The pressures at the two compression ends (P_6 and P_8) have a direct impact on the compression power consumption. In addition, the multistage mass storage process in this paper is also an optimization study of the compressor section. Therefore, in this section, a four-stage mass storage SC is studied and a cycle model is used to evaluate the influence of the outlet pressures of the compressor and pump.

Fig. 12 displays the variation of cycle efficiency with P_6 and P_8. It can be seen that all five curves show an increasing and then decreasing trend at constant P_8, reaching a maximum at around 7.6 MPa. It is also found that with constant P_6, the efficiency increases significantly with increasing P_8, while the increment becomes progressively smaller. This is because a larger P_8 will result in greater compression power consumption and poorer heat recovery from the regenerator. Meanwhile, considering that the higher the operating pressure, the higher the material requirements of equipment. Therefore, P_8 should not be too high.

Fig. 13 conducts the sensitivity analysis of P_6 and P_8 from the perspective of compressor and pump power consumption. There is no doubt that the total compression power consumption is positively correlated with P_8 under the same P_6. When P_8 is constant, the increase of P_6 yields an interesting phenomenon. Increasing P_6 makes the power consumption of the compressor increase while the power consumption of the pump decreases. However, the total power consumption decreases first and then increases. And it approximately reaches the minimum value when P_6 is 7.6 MPa. In other words, better cycle performance can be achieved when the working fluid is compressed to a value slightly above the critical pressure in the compressor. This intermediate pressure should not be too high, as the energy consumption of gaseous compression is greater than that of quasi-liquid compression. Similarly, the pressure should not be too low, as the cooling process after compression should avoid the saturated area as much as possible [28]. The change in compression power consumption precisely explains why the efficiency reaches the maximum value near $P_6 = 7.6$ MPa.

5. Summary and prospect

In this paper, the multistage mass storage process is applied to the compression process of a semi-closed S–CO_2 cycle. The process allows for more stages of compression by optimizing the cooling process, making the cooling process close to isothermal heat rejection. Therefore, thermodynamically speaking, the multistage mass storage process is not limited to SC application, but can be extended to other compression fields involving variable temperature heat rejection processes, such as all kinds of Brayton cycle system, compressed air energy storage, carbon capture and high-pressure natural gas pipeline transportation. The advantages of the multistage mass storage process are particularly considerable in applications with high-pressure ratio and high flow rate.

This paper proves that the multistage mass storage process not only reduces the loss of heat rejection process, but also brings considerable performance gains. As the number of compression/mass storage stages increases, this advantage becomes more and more obvious. However, in the actual power plant configuration, more stages mean greater system complexity and cost, in which the application of multistage mass storage process is limited. Thus there is a restrictive relationship between cost and efficiency. This paper focuses on putting forward the concept of multistage mass storage process and proves its advantages in reducing losses and improving efficiency. The technical and economic

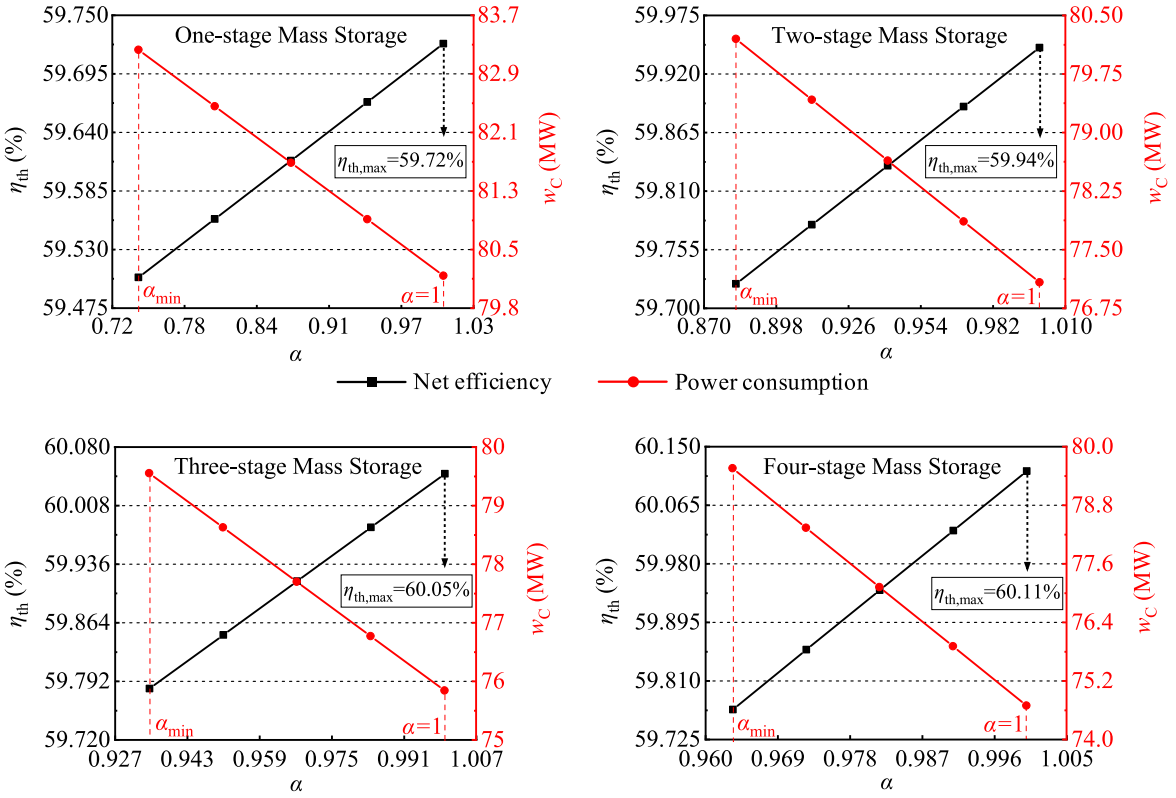

Fig. 11. Influence of split ratio on cycle performance in different cases.

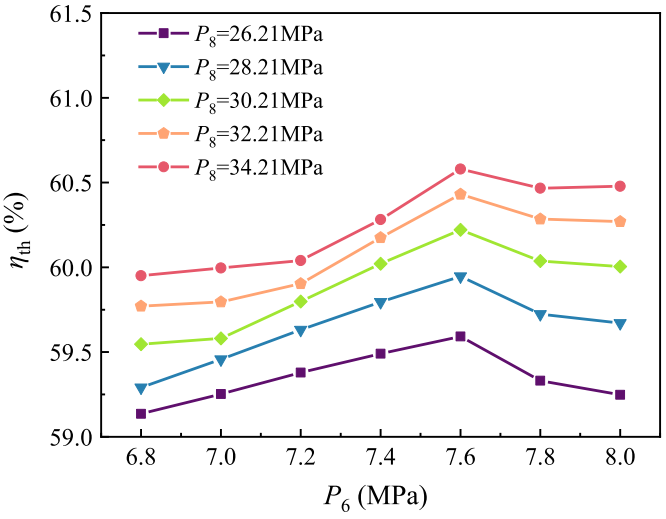

Fig. 12. Influence of P_6 and P_8 on cycle efficiency.

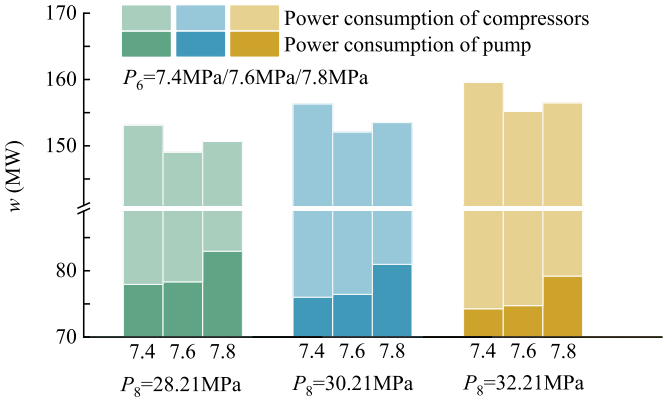

Fig. 13. Influence of P_6 and P_8 on power consumption.

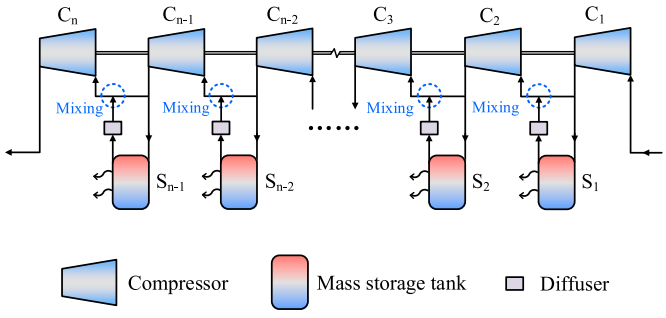

Fig. 14. Schematic diagram of improved Multi-MS.

characteristics of this new process will be studied in future work.

Furthermore, the structural form of the multistage mass storage process shown in Fig. 2 can be further improved. In order to solve the problem of mismatched pressure of confluence streams due to the pressure drop in the mass storage tank, the compression process is completed by two sets of compressors. However, the complexity of the system increases to some extent. In this regard, Fig. 14 shows an improved multistage mass storage process. Compared with Figs. 2 and 14 has one less set of compressors and an additional diffuser at the outlet of each mass storage tank. The working parameters of the compressors are the same as those of group B compressors in Fig. 2. After compression, the working fluid is split. One part enters the storage tank for slow

cooling, while the other part participates in the confluence process. Due to the pressure drop in the tank, the low-temperature fluid at the outlet of the tank needs to be pressurized to the pressure before the slow cooling by means of a diffuser. It can be seen that the improved multistage mass storage process still remains the advantages of slow cooling and mixing cooling. Compared with the form before improvement, it simplifies the complexity of the system while maintaining the original working principle. The research on the improved multistage mass storage process will be further supplemented in the following work.

6. Conclusions

In this paper, the multistage mass storage process is proposed to make the semi-closed S–CO_2 cycle achieve near-isothermal heat rejection, which can effectively reduce the compression power consumption and improve the cycle efficiency. The following conclusions are drawn.

1. The multistage mass storage process retains the characteristics of reducing power consumption through multistage compression in intercooling, while using a mass storage tank instead of cooler and applying the “storage” and “release” of working fluid in the CAES technology to the interstage cooling process. This treatment achieves a long time cooling and reduces the heat exchange loss. Thus, the mass storage process has the potential to construct the multistage mass storage, which gets rid of the restriction of the number of stages and makes the heat rejection process closer to isothermal.
2. The multistage mass storage process also presents considerable performance advantages. Compared to the SC with single-compression, the compression power consumption of the SC with four-stage mass storage is reduced by 16.47 MW, resulting in a 1.17% improvement in cycle efficiency. The efficiency of the SC with one-stage mass storage is even 0.15% higher than that of the SC with two-stage intercooling when compared to an intercooling process with the same performance advantage principle.
3. The multistage mass storage is compared qualitatively with intercooling and CAES, respectively. In contrast to intercooling, the cooling methods of the multistage mass storage process are slow cooling and mixing cooling rather than the direct cooling of intercooling. While compared to CAES, the compression heat of the multistage mass storage process is released directly to the environment rather than reused. The differences between them are also reflected in the different mechanical energy flows and the location of the storage tank application.
4. The thermodynamic principle of the multistage mass storage process is to make the heat rejection process of the cycle approach isothermal. Therefore, it has the potential to be applied in a variety of compression fields involving variable temperature heat rejection process, such as all kinds of Brayton cycle systems, carbon capture and high-pressure natural gas pipeline transportation.

Credit author statement

Enhui Sun: Visualization, Theory. Hongfu Ji: Methodology, Simulation. Xiangren Wang: Investigation. Wenjing Ma: Data curation. Lei Zhang: Writing- Reviewing and Editing. Jinliang Xu: Supervision.

Declaration of competing interest

The authors declare that they have no known competing financial interests or personal relationships that could have appeared to influence the work reported in this paper.

Data availability

No data was used for the research described in the article.

Acknowledgements

The research was supported by the Natural Science Foundation of China (52206010, 52076079), the Fundamental Research Funds for the Central Universities (2021MS076).

Appendix A

For several intercooling and mass storage procesendix A displays the values of temperature, pressure and mass flow at their state points. Table A1 shows the One-Ic and Two-Ic, and Table A2 shows the One-MS, Two-MS, Three-MS and Four-MS.

Table A1
State parameter points of intercooling process (refer to Fig. 6(a))

	One-Ic			Two-Ic		
Point	T (°C)	P (MPa)	m (kg/s)	T (°C)	P (MPa)	m (kg/s)
1_{ic}	27	3.27	1851	27	3.27	1851
2_{ic}	61.39	4.92	1851	49.65	4.29	1851
3_{ic}	27	4.78	1851	27	4.15	1851
4_{ic}	63.78	7.4	1851	52.51	5.64	1851
5_{ic}				27	5.50	1851
6_{ic}				51.31	7.4	1851

Table A2
State parameter points of mass storage process (refer to Fig. 2(a))

	One-MS (n = 2)			Two-MS (n = 3)			Three-MS (n = 4)			Four-MS (n = 5)		
Point	T (°C)	P (MPa)	m (kg/s)	T (°C)	P (MPa)	m (kg/s)	T (°C)	P (MPa)	m (kg/s)	T (°C)	P (MPa)	m (kg/s)
$C_{1,in}$	27	3.27	1850.12	27	3.27	1850.12	27	3.27	1850.12	27	3.27	1850.12
$C_{1,out}$	63.84	5.06	1850.12	52.39	4.43	1850.12	46.78	4.15	1850.12	43.45	3.99	1850.12
$S_{1,out}$	18	4.92	2.5896	18	4.29	1.93	18	4.01	1.50	18	3.85	1.22
$C_{2,in}$	18	4.92	1847.53	18	4.29	1848.19	18	4.01	1848.62	18	3.85	1848.90

(continued on next page)

Table A2 (*continued*)

	One-MS (n = 2)			Two-MS (n = 3)			Three-MS (n = 4)			Four-MS (n = 5)		
Point	T (°C)	P (MPa)	m (kg/s)	T (°C)	P (MPa)	m (kg/s)	T (°C)	P (MPa)	m (kg/s)	T (°C)	P (MPa)	m (kg/s)
$C_{2,out}$	50.97	7.4	1847.53	42.1	5.78	1848.19	36.80	5.06	1848.62	33.65	4.67	1848.90
$S_{2,out}$				18	5.64	4.62	18	4.92	3.67	18	4.53	2.75
$C_{3,in}$				18	5.64	1843.57	18	4.92	1844.95	18	4.53	1846.15
$C_{3,out}$				38.58	7.4	1843.57	36.05	6.17	1844.95	33.15	5.48	1846.15
$S_{3,out}$							18	6.03	7.37	18	5.34	5.59
$C_{4,in}$							18	6.03	1837.58	18	5.34	1840.56
$C_{4,out}$							33.64	7.4	1837.58	32.34	6.42	1840.56
$S_{4,out}$										18	6.28	13.56
$C_{5,in}$										18	6.28	1827
$C_{5,out}$										32.46	7.4	1827
$C_{n+1,in}$	27	3.27	0.88	27	3.27	0.88	27	3.27	0.88	27	3.27	0.88
$C_{n+1,out}$	61.39	4.92	0.88	49.65	4.29	0.88	43.88	4.01	0.88	40.46	3.85	0.88
$C_{n+2,in}$	27	4.92	3.47	27	4.29	2.81	27	4.01	2.38	27	3.85	2.1
$C_{n+2,out}$	61.19	7.4	3.47	49.66	5.64	2.81	43.90	4.92	2.38	40.47	4.53	2.1
$C_{n+3,in}$				27	5.64	7.43	27	4.92	6.05	27	4.53	4.85
$C_{n+3,out}$				49.09	7.4	7.43	43.79	6.03	6.05	40.44	5.34	4.85
$C_{n+4,in}$							27	6.03	13.42	27	5.34	10.44
$C_{n+4,out}$							43.14	7.4	13.42	40.27	6.28	10.44
$C_{n+5,in}$										27	6.28	24
$C_{n+5,out}$										39.62	7.4	24

Note: ''in'' and ''out'' represent inlet and outlet, respectively; S_{out} refers to the outlet stream mixed with the group B compressors.

Appendix B

Table B makes a detailed performance comparison of the S-Compr cycle, intercooling cycle and mass storage cycle mentioned in the paper, especially the power consumption of the compressors in each case.

Table B
Performance comparison of several cycle cases

Cases	Power consumption of compressor (MW)										Net power (MW)	η_{th} (%)
S-Compr						91.23					827.94	58.94
Intercooling			Compr 1_{ic}			Compr 2_{ic}			Compr 3_{ic}			
One-Ic			43.54			40.82					834.81	59.43
Two-Ic			28.59			29.88			23.89		836.82	59.57
Mass storage	C_1	C_2	C_3	C_4	C_5	C_{n+1}	C_{n+2}	C_{n+3}	C_{n+4}	C_{n+5}		
One-MS (n = 2)	46.66	33.45				0.0207	0.0701				838.98	59.72
Two-MS (n = 3)	32.06	26.27	18.63			0.0136	0.0398	0.0895			842.08	59.94
Three-MS (n = 4)	24.94	21.12	18.15	11.25		0.0101	0.0257	0.0596	0.1124		843.50	60.05
Four-MS (n = 5)	20.72	17.87	15.99	13.54	6.339	0.0081	0.0183	0.0397	0.0777	0.1516	844.41	60.11

Q = 1404.8 MW, w_T = 999.46 MW, w_P = 80.29 MW.

References

[1] Allam RJ, Palmer MR, Brown GW, Fetvedt J, Freed D, Nomoto H, et al. High efficiency and low cost of electricity generation from fossil fuels while eliminating atmospheric emissions, including carbon dioxide. Energy Proc 2013;37:1135–49.

[2] Wang K, Wang S. Thermodynamic analysis of a comprehensive energy utilization system for natural gas pressure reduction stations based on Allam cycle. Appl Therm Eng 2022;205:118033.

[3] Zheng Y, Gao L, He S. Analysis of the mechanism of energy consumption for CO_2 capture in a power system. Energy 2023;262:125103.

[4] Dokhaee E, Saraei A, Jafari Mehrabadi S, Yousefi P. Simulation of the Allam cycle with carbon dioxide working fluid and comparison with Brayton cycle. Int J Energy Environ Eng 2021;12:543–50.

[5] Sleiti AK, Al-Ammari W, Ahmed S, Kapat J. Direct-fired oxy-combustion supercritical-CO_2 power cycle with novel preheating configurations-thermodynamic and exergoeconomic analyses. Energy 2021;226:120441.

[6] Weiland NT, White CW. Techno-economic analysis of an integrated gasification direct-fired supercritical CO_2 power cycle. Fuel 2018;212:613–25.

[7] Zhao Y, Yu B, Wang B, Zhang S, Xiao Y. Heat integration and optimization of direct-fired supercritical CO_2 power cycle coupled to coal gasification process. Appl Therm Eng 2018;130:1022–32.

[8] Luo J, Emelogu O, Morosuk T, Tsatsaronis G. Exergy-based investigation of a coal-fired allam cycle. Energy 2021;218:119471.

[9] Ishii H, Hayashi T, Tada H, Yokohama K, Takashima R, Hayashi Jichiro. Critical assessment of oxy-fuel integrated coal gasification combined cycles. Appl Energy 2019;233–234:156–69.

[10] Penkuhn M, Tsatsaronis G. Systematic evaluation of efficiency improvement options for sCO_2 Brayton cycles. Energy 2020:210.

[11] Tyagi SK, Chen GM, Wang Q, Kaushik SC. Thermodynamic analysis and parametric study of an irreversible regenerative-intercooled-reheat Brayton cycle. Int J Therm Sci 2006;45:829–40.

[12] Sun E, Ji H, Ma W, Xu J, Zhang L, Wang Y. Development of an analytical constituent split method to analyze a semi-closed supercritical carbon dioxide power cycle. Energy Convers Manag 2022;254:115261.

[13] Zhou J, Zhang C, Su S, Wang Y, Hu S, Liu L, et al. Exergy analysis of a 1000MW single reheat supercritical CO_2 Brayton cycle coal-fired power plant. Energy Convers Manag 2018;173:348–58.

[14] Allam RJ, Fetvedt JE, Forrest BA, Freed DA. The oxy-fuel, supercritical CO_2 Allam cycle: new cycle developments to produce even lower-cost electricity from fossil fuels without atmospheric emissions. In: ASME Turbo Expo 2014: turbine technical conference and exposition. American Society of Mechanical Engineers; 2014.

[15] Chan W, Lei X, Chang F, Li H. Thermodynamic analysis and optimization of Allam cycle with a reheating configuration. Energy Convers Manag 2020;224:113382.

[16] Bejan Adrian. Advanced engineering thermodynamics. Advanced engineering thermodynamics; 1988.

[17] Ma Y, Liu M, Yan J, Liu J. Thermodynamic study of main compression intercooling effects on supercritical CO_2 recompression Brayton cycle. Energy 2017;140:746–56.

[18] Linares JI, Montes MJ, Cantizano A, Sánchez C. A novel supercritical CO_2 recompression Brayton power cycle for power tower concentrating solar plants. Appl Energy 2020;263:114644.

[19] Lugo-Méndez H, Lopez-Arenas T, Torres-Aldaco A, Torres-González EV, Sales-Cruz M, Lugo-Leyte R. Interstage pressures of a multistage compressor with intercooling. Entropy 2021;23:1–14.

[20] Weiland N, Shelton W, White C, Gray D. Performance baseline for direct-fired sCO_2 cycles. 5th Int Supercrit CO_2 Power Cycles Symp 2016:1–18.

[21] Mondal S, De S. CO_2 based power cycle with multi-stage compression and intercooling for low temperature waste heat recovery. Energy 2015;90:1132–43.

[22] Zhu HH, Wang K, He YL. Thermodynamic analysis and comparison for different direct-heated supercritical CO_2 Brayton cycles integrated into a solar thermal power tower system. Energy 2017;140:144–57.

[23] Wang K, He YL, Zhu HH. Integration between supercritical CO_2 Brayton cycles and molten salt solar power towers: a review and a comprehensive comparison of different cycle layouts. Appl Energy 2017;195:819–36.
[24] Padilla RV, Soo Too YC, Benito R, Stein W. Exergetic analysis of supercritical CO_2 Brayton cycles integrated with solar central receivers. Appl Energy 2015;148:348–65.
[25] Haseli Y, Sifat NS. Performance modeling of Allam cycle integrated with a cryogenic air separation process. Comput Chem Eng 2021;148:107263.
[26] Maheshwari M, Singh O. Thermo-economic analysis of combined cycle configurations with intercooling and reheating. Energy 2020;205:118049.
[27] Carchedi F, Wood GR. Design and development of a 12:1 Pressure ratio compressor for the ruston 6-MW gas turbine. J Eng Gas Turbines Power 1982;104:823–31.
[28] Zhao Y, Wang B, Chi J, Xiao Y. Parametric study of a direct-fired supercritical carbon dioxide power cycle coupled to coal gasification process. Energy Convers Manag 2018;156:733–45.
[29] Lu X, Beauchamp D, Laumb J, Stanislowski J, Swanson M, Dunham D, et al. Coal drying study for a direct syngas fired supercritical CO_2 cycle integrated with a coal gasification process. Fuel 2019;251:636–43.
[30] White CW, Weiland NT. Evaluation of property methods for modeling direct-supercritical CO_2 power cycles. J Eng Gas Turbines Power 2018;140.
[31] Li XH, Deng TR, Ma T, Ke HB, Wang QW. A new evaluation method for overall heat transfer performance of supercritical carbon dioxide in a printed circuit heat exchanger. Energy Convers Manag 2019;193:99–105.
[32] Maheshwari M, Singh O. Thermodynamic study of different configurations of gas-steam combined cycles employing intercooling and different means of cooling in topping cycle. Appl Therm Eng 2019;162:114249.
[33] Rogalev A, Grigoriev E, Kindra V, Rogalev N. Thermodynamic optimization and equipment development for a high efficient fossil fuel power plant with zero emissions. J Clean Prod 2019;236:117592.
[34] Zhu M, Zhou J, Chen L, Su S, Hu S, Qing H, et al. Economic analysis and cost modeling of supercritical CO_2 coal-fired boiler based on global optimization. Energy 2022;239:122311.
[35] Xue X, Lv J, Chen H, Xu G, Li Q. Thermodynamic and economic analyses of a new compressed air energy storage system incorporated with a waste-to-energy plant and a biogas power plant. Energy 2022;261:125367.
[36] Guo H, Xu Y, Huang L, Zhu Y, Liang Q, Chen H. Concise analytical solution and optimization of compressed air energy storage systems with thermal storage. Energy 2022;258:124773.
[37] Guo H, Xu Y, Zhang X, Zhou X, Chen H. Transmission characteristics of exergy for novel compressed air energy storage systems-from compression and expansion sections to the whole system. Energy 2020;193:116798.
[38] Chen L, Zheng T, Mei S, Xue X, Liu B, Lu Q. Review and prospect of compressed air energy storage system. J Mod Power Syst Clean Energy 2016;4:529–41.
[39] Scaccabarozzi R, Gatti M, Martelli E. Thermodynamic analysis and numerical optimization of the NET Power oxy-combustion cycle. Appl Energy 2016;178:505–26.
[40] Chan W, Li H, Li X, Chang F, Wang L, Feng Z. Exergoeconomic analysis and optimization of the Allam cycle with liquefied natural gas cold exergy utilization. Energy Convers Manag 2021:235.
[41] Krail J, Beckmann G, Schittl F, Piringer G. Comparative thermodynamic analysis of an improved ORC process with integrated injection of process fluid. Energy 2023;266:126352.
[42] Luo J, Lu P, Chen K, Luo X, Chen J, Liang Y, et al. Experimental and simulation investigation on the heat exchangers in an ORC under various heat source/sink conditions. Energy 2023;264:126189.
[43] Lemmon EW, Huber ML, McLinden MO. NIST standard reference database 23: reference fluid thermodynamic and transport properties-REFPROP. Version 9.0. Gaithersburg: National Institute of Standards and Technology, Standard Reference Data Program; 2010.
[44] Cengel YA, Boles MA. Thermodynamics: an engineering approach. Thermodynamics: An Engineering Approach; 2009.
[45] Sun E, Xu J, Li M, Li H, Liu C, Xie J. Synergetics: the cooperative phenomenon in multi-compressions S-CO_2 power cycles. Energy Convers Manag X 2020;7:100042.
[46] Cheng WL, Huang WX, Nian Y Le. Global parameter optimization and criterion formula of supercritical carbon dioxide Brayton cycle with recompression. Energy Convers Manag 2017;150:669–77.
[47] Zhang Y, Yang K, Hong H, Zhong X, Xu J. Thermodynamic analysis of a novel energy storage system with carbon dioxide as working fluid. Renew Energy 2016;99:682–97.